

Magneto-dielectric characterization of TiO₂-CoFe₂O₄ derived ceramic composites

Original

Magneto-dielectric characterization of TiO₂-CoFe₂O₄ derived ceramic composites / Galizia, Pietro; Baldisserri, Carlo; Galassi, Carmen; Maizza, Giovanni; Anbinderis, Maksimas; Grigalaitis, Robertas; Banyas, Juras. - In: PROCESSING AND APPLICATION OF CERAMICS. - ISSN 1820-6131. - STAMPA. - 12:4(2018), pp. 350-356.
[10.2298/PAC1804350G]

Availability:

This version is available at: 11583/2746252 since: 2019-08-05T18:47:55Z

Publisher:

Novi sad, Serbia

Published

DOI:10.2298/PAC1804350G

Terms of use:

This article is made available under terms and conditions as specified in the corresponding bibliographic description in the repository

Publisher copyright

(Article begins on next page)



Magneto-dielectric characterization of $\text{TiO}_2\text{-CoFe}_2\text{O}_4$ derived ceramic composites

Pietro Galizia^{1,2,*}, Maksimas Anbinderis³, Robertas Grigalaitis³, Juras Banys³, Carlo Baldisserrì¹, Giovanni Maizza², Carmen Galassi¹

¹CNR - ISTECE, Via Granarolo 64, I-48018 Faenza, Italy

²Department of Applied Science and Technology (DISAT), Polytechnic University of Turin, C.so Duca degli Abruzzi 24, I-10129 Torino, Italy

³Vilnius State University, Faculty of Physics, LT-10222 Vilnius, Lithuania

Received 10 June 2018; Received in revised form 4 October 2018; Accepted 20 November 2018

Abstract

Dielectric permittivity (ϵ'), magnetic permeability (μ') and dielectric and magnetic loss ($\tan \delta_\epsilon$ and $\tan \delta_\mu$, respectively) of magneto-dielectric cobalt ferrite-titania (CFO-TO) ceramic composites are determined from 200 to 300 MHz. The four different combinations of phases - that can be produced in the sintered composite, according to the starting CFO/TO molar ratio - allow to tune the macroscopic permittivity and permeability. For the first time impedance, miniaturization and magneto-dielectric loss of the four classes of composites are calculated and discussed. The displayed miniaturization factors between 4.4 and 8.2 in the very-high frequency (VHF) range corroborate their potential application as magneto-dielectric substrate materials for antennas. Remarkably, the ceramic composites characterized by 2 vol.% and 3 vol.% of CFO and TO, respectively, dispersed in $\text{Fe}_2\text{CoTi}_3\text{O}_{10}$ (FCTO) matrix display a magneto-dielectric loss lower than 0.07 and a miniaturization factor of 4.8.

Keywords: composites, ferrites, titanates, dielectric properties, magnetic properties

1. Introduction

The possibility of easily tuning or enhancing certain properties of multifunctional materials paves the way for new applications [1]. Composite materials answer to this technological demand [2–4], and increasing efforts are being focused on ferrites and their composites with dielectric, ferroelectric, and optoelectronic materials. Among such materials, magneto dielectrics (MDs) show properties that can easily be tuned, as required in the case of substrates for miniaturized antennas [5]. In particular, MDs allow to tune their permeability and permittivity values as demanded by the working frequency range, while keeping low loss [6–8].

By combining a relative magnetic permeability (μ_r) greater than unity with a reasonably low value of relative dielectric permittivity (ϵ_r) it is possible to achieve a favourable miniaturization factor [$n = (\mu_r \cdot \epsilon_r)^{1/2}$] with-

out affecting the radiating properties. However, reducing the magnetic and dielectric loss at the same time is still a challenge [9–11]. It is well-known that ferrites are the best candidates for antenna substrates and a number of compositions have been investigated, including spinel ferrites and hexagonal ferrites, in some cases combined with other ceramics. Zheng *et al.* [12] were able to reduce loss by combining NiZn ferrite with Ba hexaferrite, or Co-Zn hexaferrite [13], bringing the ϵ_r/μ_r ratio down to about one over a wide frequency range (1–10² MHz). Two-step sintering allowed to obtain very low magnetic and dielectric loss tangent [14], while improved magneto-dielectric effect was found by Banerjee *et al.* [15] in composites of NiZn ferrite nanoparticles with BaTiO_3 , synthesized by a chemical method.

Magnetic/dielectric properties of ceramic composites can be tuned by tailoring composition, interconnectivity and interfaces. Overall properties of the composite may follow the rule of mixtures as well as more complex combinations of the properties of the side phases,

*Corresponding authors: tel: +39 0546 699777,
e-mail: pietro.galizia@istec.cnr.it

or may be dominated by one or more phases of the composite [16]. Moreover, even a limited interaction between the two components of a binary ceramic composition may cause novel properties to appear, which were absent in both components [17–19].

In search for new candidates for magneto-dielectric materials, we studied the system cobalt ferrite (CoFe_2O_4 , CFO) and titanium oxide (TiO_2 , TO), owing to high coercivity, and moderate magnetic moment of the CFO, and low eddy current and dielectric loss of TO [20–25]. However, ceramic composites based on the binary system $\text{TiO}_2/\text{CoFe}_2\text{O}_4$ are sintered at temperatures lower than about 600°C , in order to avoid the anatase-to-rutile transformation [26] which generally reduces the photocatalytic properties. To the best of our knowledge, there is scanty literature about the properties of the $\text{Fe}_2\text{CoTi}_3\text{O}_{10}$ (FCTO) compound resulting from the reaction between CFO and TO at temperature higher than 800°C [7,27,28].

In this work, we focus on the dielectric and magnetic characterization of *in situ* synthesized ceramic composites derived from displacement reactions between TiO_2 and CoFe_2O_4 . By using *in situ*, we intend to contrast these materials with the more conventional composites, in which the side phases are the same as the final ones, the materials being obtained starting from TiO_2 and CoFe_2O_4 powder mixtures. By exploiting the displacement reactions (i.e. by changing the starting TO/CFO molar ratio) four different phases mixtures can be produced [27]: i) TO + FCTO, for TO/CFO starting molar ratio higher than 3; ii) FCTO + TO + CFO, for TO/CFO starting molar ratio equal to 3; iii) FCTO + CFO, for $1-2 < \text{TO/CFO} < 3$ (in fact the lower bound has never been investigated [29]); and iv) CFO + CoTiO_3 + Fe_2O_3 , for $0 < \text{TO/CFO} < 0.8-1$ (the upper bound has never been investigated [29]). *In situ* synthesized ceramic composites provide good trade-off between dielectric/magnetic constants and dielectric/magnetic loss and allow to optimize their intrinsic impedance and magneto-dielectric efficiency for their possible application as antenna substrates in the very-high frequency (VHF) range.

II. Materials and methods

Cobalt ferrite-titania ceramic composites are produced by conventional sintering at 1200°C starting from mixtures of said phases (cobalt ferrite, CFO and titania, TO), according to the compositional scheme $(100-x)\text{TO}-x\text{CFO}$, with $x = 20, 49.5, 57$ and 80 wt.%. In Table 1 the correlation between samples' IDs, starting

CFO content, and final composition of the samples is reported. Further details on powder's synthesis, densification and microstructural features of the produced samples are reported in a previously published work [27].

The microstructure of the sintered samples is investigated on polished cross section by SEM (Quanta, FEI).

For dielectric measurements over the 200–300 MHz frequency range, the samples are prepared by applying Ag electrodes onto the polished surfaces of properly machined cylinders and placed at the end of short-circuited coaxial line between the inner conductor and the terminating contact. Measurements are performed using an Agilent 8714ET network analyser. The complex reflection coefficient of the electromagnetic wave is measured and the dielectric permittivity is calculated using the parallel-plate capacitor formula:

$$\varepsilon^* = \frac{(C^* - C_0) \cdot d}{\varepsilon_0 \cdot A} \quad (1)$$

where C is the complex capacitance of the sample, d is its thickness, A is the area of the sample and $\varepsilon_0 = 8.85 \cdot 10^{-12} \text{ F/m}$ is the permittivity of free space. Capacitance C_0 is estimated by measuring an air gap of length d . Magnetic measurements of the ceramic composites over the 200–300 MHz frequency range are performed by applying the inductance measurement method. A 3 mm diameter hole is machined in the centre of disk-shaped ceramics having external diameter 9 mm and thickness 3.1 mm for CFT20, and 4.8 mm for the others. The ring-shaped samples are mounted into a measurement test fixture forming an ideal (no magnetic flux leakage) one-turn inductor which is placed in an home-made sample holder (analogous to the Agilent 16454A magnetic test fixture [29]), which is connected to the Agilent E8363B network analyser. The complex relative permeability is calculated from the measured complex impedance values using the formula:

$$\mu^* = \frac{2\pi \cdot (Z_m^* - Z_s^*)}{j \cdot \omega \cdot \mu_0 \cdot h \ln \frac{R}{r}} + 1 \quad (2)$$

Here Z_m and Z_s denote the impedance of the measurement cell with and without the sample, respectively, R and r are the outer and inner radii of the ring-shaped sample, h is its thickness, and μ_0 is the magnetic permeability of free space.

III. Results and discussion

In Fig. 1 the microstructure of the produced samples is shown. The different phases are evidenced by

Table 1. Compositions of the ceramic composites [27]

Sample ID	Starting composition CFO [wt.%]	Final composition [vol.%]					
		CFO	TO	FCTO	CTO	FO	Porosity
CFT20	20.0	0	60	39	0	0	1
FCTO	49.5	2	3	90	0	0	5
CFT57	57.0	12	0	83	0	0	5
CFT80	80.0	19	0	0	37	36	8

different grey scale according to their density (i.e. the phases with higher density show pale grey that darkens with decreasing density). Hence, in case of the CFT20, Fig. 1a, the black areas are pores (as for all the other samples), the darker grains are TiO_2 (rutile, density, $\rho = 4.25 \text{ g/cm}^3$), and the brighter grains are $\text{Fe}_2\text{CoTi}_3\text{O}_{10}$ ($\rho = 4.31 \text{ g/cm}^3$). For the FCTO sample, Fig. 1b, the darker grains are TiO_2 , those displaying medium grey are $\text{Fe}_2\text{CoTi}_3\text{O}_{10}$, and the brighter ones are CoFe_2O_4 ($\rho = 5.30 \text{ g/cm}^3$). In case of the CFT57, Fig. 1c, the darker grains are $\text{Fe}_2\text{CoTi}_3\text{O}_{10}$, and the brighter ones are CoFe_2O_4 . For the CFT80 it is more difficult to distinguish the phases, even if, in principle, the darker grains are CoTiO_3 ($\rho = 4.98 \text{ g/cm}^3$), those displaying medium grey are Fe_2O_3 (hematite, $\rho = 5.27 \text{ g/cm}^3$), and the brighter ones are CoFe_2O_4 .

In Fig. 2a the spectra for the real permeability μ' are shown. In the investigated frequency range, all the μ' curves display the typical trend of a plateau below a certain frequency and the distinct peaking behaviour that is modelled by Snoek's law [30].

As expected, higher μ' values are shown by the samples with the highest amount of CFO, i.e. CFT80 and CFT57 display permeability value of 1.22 and 1.16, respectively. These compounds show the highest μ'' values too (Fig. 2b). Even though the FCTO has 2 vol.% of CFO, its μ' spectra is comparable with the dielectric CFT20. This could be attributed to the microstructure

and shape of the CFO grains [31–34]. In fact, the small amount of CFO in the FCTO sample, compared to the CFT80 and CFT57 samples, allows the development of smaller CFO grains [27], which, on the one hand reduce the contribution of the domain-wall motion [22,33,34], and on the other hand enhance spin rotation owing to the higher weight of surface's effects. It is worth noting that spin rotation is an intrinsic property of the bulk material, but in material's surface it is influenced by extrinsic properties such as grain size and shape [35]. Anyway, spin rotation contribution is not negligible, since the ferromagnetic resonance is expected at higher frequencies (about 2–4 GHz [36]).

The frequency dependence of permittivity ε' and dielectric loss tangent ($\tan \delta_\varepsilon$) are shown in Fig. 3. It can be seen that for the heterostructures containing TO and/or FCTO components the dielectric permittivity is almost constant over the whole analysed frequency range, and its average value decreases with decreasing the titania content. The permittivity of FCTO is normally lower than that of TiO_2 , so the presence of FCTO in the composites will produce a dilution effect. For the CFT80 sample, which has 19 vol.% CFO and 36 vol.% Fe_2O_3 , respectively, the dielectric permittivity is higher at low frequencies and decreases with increasing frequency, as expected from the Maxwell-Wagner theory applied to ferrite-containing composites [37,38], and according to the Kramers-Kronig relations since the 12%

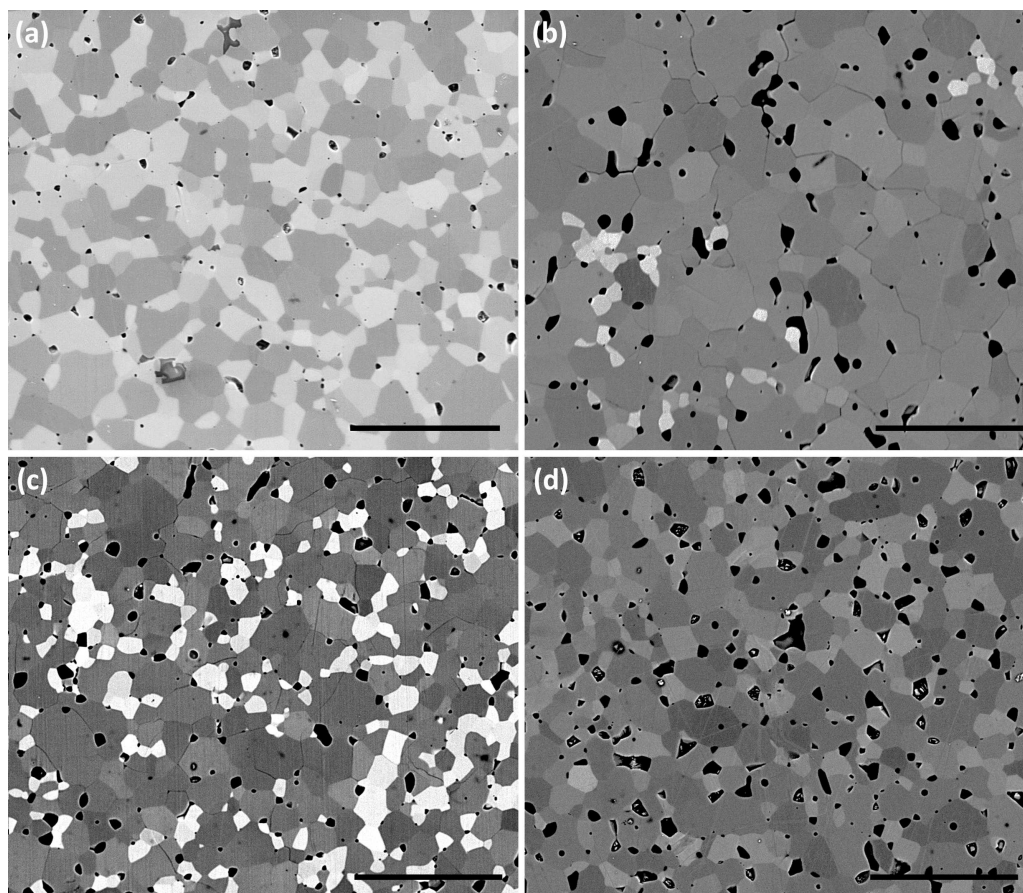


Figure 1. BSE SEM images of (a) CFT20, (b) FCTO, (c) CFT57, and (d) CFT80 (length of all bars is 20 μm)

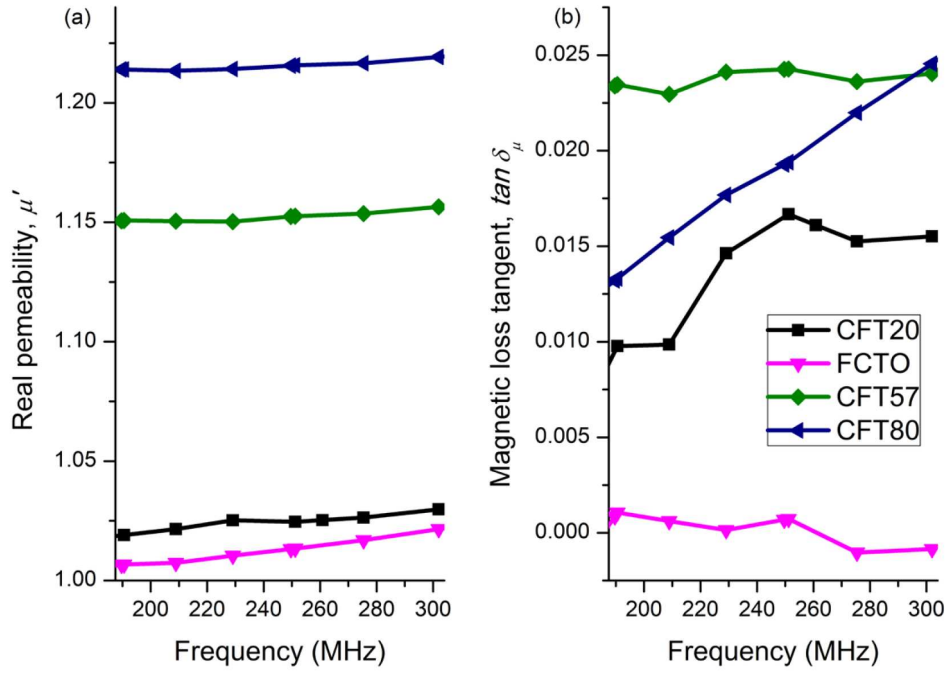


Figure 2. Real permeability μ' (a) and magnetic loss tangent ($\tan \delta_\mu$) dispersion (b) in the frequency range of 200–300 MHz

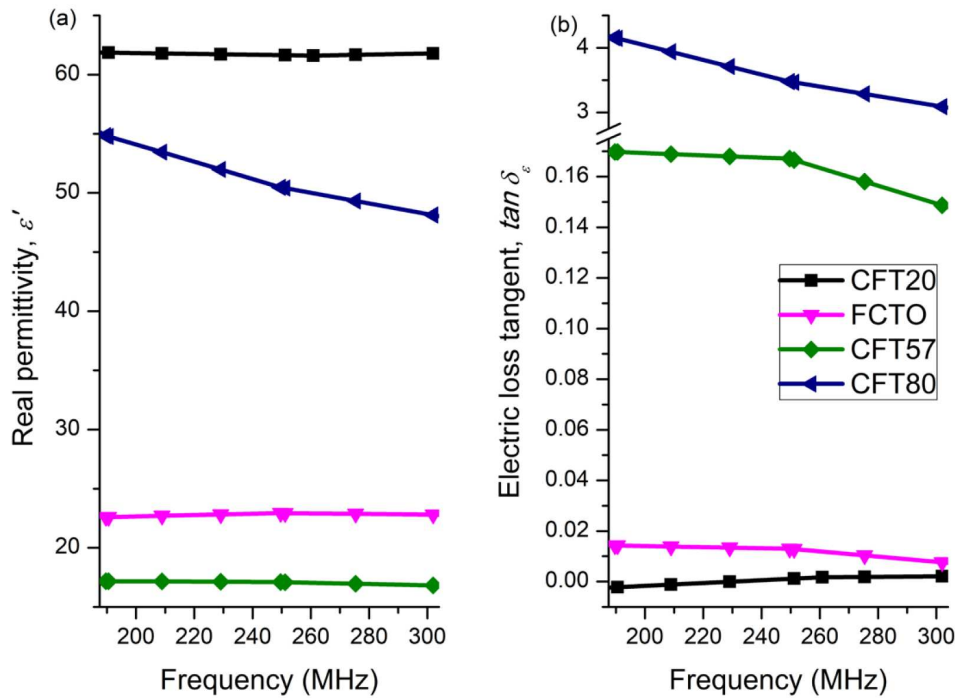


Figure 3. Real permittivity ϵ' (a) and dielectric loss tangent ($\tan \delta_\epsilon$) dispersion (b) in the frequency range of 200–300 MHz

of ϵ' reduction is accompanied by high loss ($\tan \delta_\epsilon > 3$). The dielectric loss tangent ($\tan \delta_\epsilon$) of the CFT20 and FCTO samples is negligibly small and remains stable in the whole frequency range. Titania significantly flattens both ϵ' and $\tan \delta_\epsilon$ curves. The $\tan \delta_\epsilon$ values of samples can be correlated with the amount of porosity (Table 1) because $\tan \delta_\epsilon$ values grow with increasing porosity. The increase of a few orders of magnitude of $\tan \delta_\epsilon$ in the CFT80 sample, beside porosity contribution, can be due to its complex microstructure which promotes the

accumulation of free charge carriers at the interfaces between the magnetic and dielectric phases causing the so-called space charge polarization which can be accounted by the above mentioned Maxwell-Wagner theory. Contrary to other ferrites, where the dielectric constant is closely related to the concentration of Fe^{2+} ions [39–42], for cobalt ferrites this contribution is missing since the iron cations are stabilized in the Fe^{3+} state due to the presence of Co^{2+} .

Owing to the easily adjustable permeability and per-

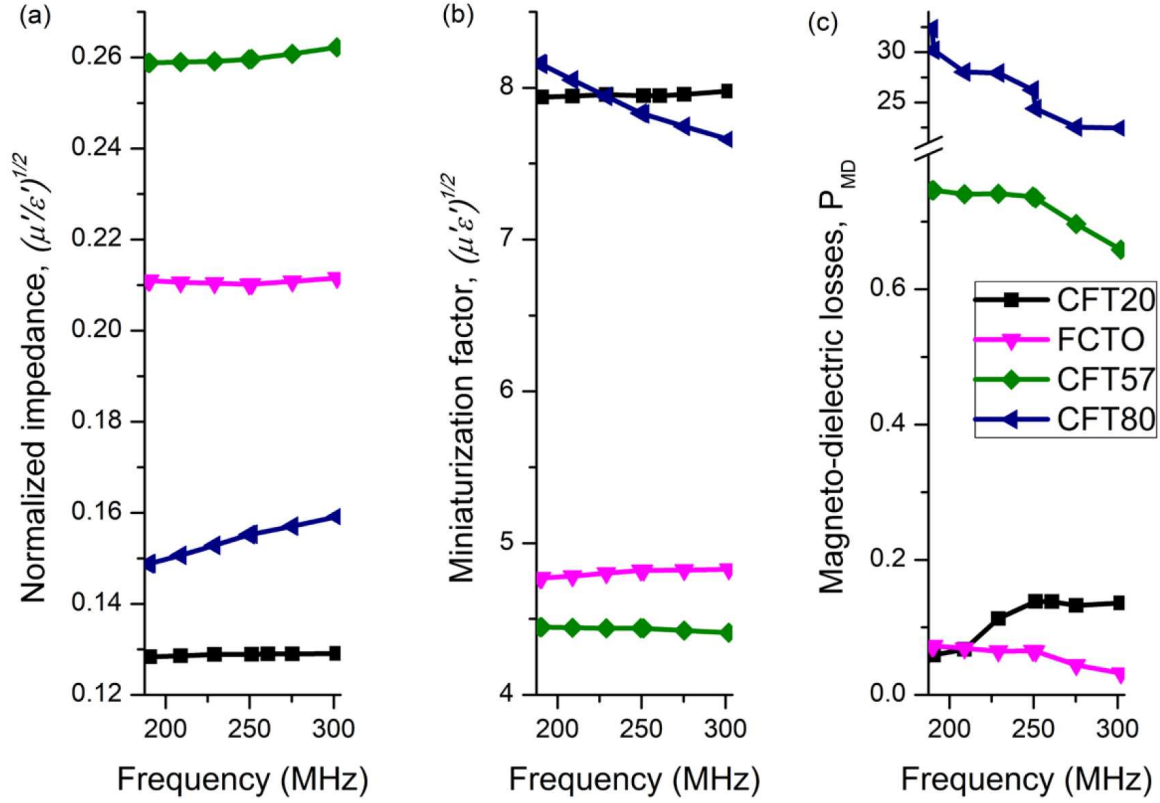


Figure 4. Normalized impedance $(\mu'/\epsilon')^{1/2}$ (a), miniaturization factor $(\mu'\epsilon')^{1/2}$ (b) and magneto-dielectric loss $P_{MD} = (\tan \delta_\mu + \tan \delta_\epsilon) \cdot (\epsilon'/\mu')^{1/2}$ (c) in the frequency range of 200–300 MHz

mittivity, the developed CFT composites can be used as a magneto-dielectric antenna substrate. The spectra of normalized impedance $(\mu'/\epsilon')^{1/2}$ and miniaturization factor $(\mu'\epsilon')^{1/2}$ are shown in Fig. 4a and 4b, respectively. It can be observed that the impedance $(\mu'/\epsilon')^{1/2}$ value for the CFT57 sample is the highest among the investigated compositions and is always higher than 0.25. On the other hand, the characteristic impedance is four times lower than the impedance of the free space. A miniaturization factor of about 8 is achieved with the samples CFT80 and CFT20. Despite the smaller miniaturization factor (about 4.5), the CFT57 sample, is also desirable for using it as a magneto-dielectric antenna substrate material [43].

Magneto-dielectric loss P_{MD} (Fig. 4c) is calculated as:

$$P_{MD} = (\tan \delta_\mu + \tan \delta_\epsilon) \sqrt{\frac{\epsilon'}{\mu'}} \quad (3)$$

where the $(\epsilon'/\mu')^{1/2}$ term is related to the stored energy. Consequently, the performances of an antenna printed on those magneto-dielectric substrates, and particularly its radiation efficiency and bandwidth will be better in materials with lower P_{MD} values [44]. In particular, FCTO composites display the lowest P_{MD} , lower than 0.07. Among the other, FCTO/CFO system seems to be the most promising and suitable for very-high-frequency applications.

IV. Conclusions

In this paper, the magneto-dielectric properties of novel titania-cobalt ferrite *in situ* synthesized ceramic composites are characterized. Due to the high reactivity of the two starting phases the final composition of the composite material changes significantly and the different microstructures result in significantly different functional properties. Therefore, the titania-cobalt ferrite system provides an accurate composition-dependent control of the microstructure and, thus, the possibility to easily tailor the magnetodielectric properties. The best compromise among magnetic permeability, dielectric permittivity and loss is achieved in the samples with the starting TO/CFO ratio 43/57 and 50.5/49.5. These samples, based on FCTO/CFO and FCTO/CFO/TO phases mixture, respectively, show a combination of properties (FCTO/CFO: $1.15 < \mu' < 1.16$, $16.9 < \epsilon' < 18.4$, $0.66 < P_{MD} < 0.75$; and FCTO/CFO/TO: $1 < \mu' < 1.02$, $22.6 < \epsilon' < 23.6$, and $0.03 < P_{MD} < 0.07$) that can be exploited for the design of miniaturized antennas for very-high-frequency applications.

Acknowledgement: The authors gratefully acknowledge the skilful contribution of Mr. C. Capiani (CNR-ISTEC) for the preparation of the samples. This work was partially supported by the ANTENNA project, contract n. 1466.

References

1. S.G. Rohrer, M. Affatigato, M. Backhaus, R.K. Bordia, H.M. Chan, S. Curtarolo, A. Demkov, J.N. Eckstein, K.T. Faber, J.E. Garay, Y. Gogotsi, L. Huang, L.E. Jones, S.V. Kalinin, R.J. Lad, C.G. Levi, J. Levy, J.-P. Maria, L. Matos Jr., A. Navrotsky, N. Orlovskaya, C. Pantano, J.F. Stebbins, T.S. Sudarshan, T. Tani, K. Scott Weil, “Challenges in ceramic science: A report from the workshop on emerging research areas in ceramic science”, *J. Am. Ceram. Soc.*, **95** (2012) 3699–3712.
2. M. Taya, *Electronic Composites: Modelling, Characterization, Processing, MEMS Application*, Cambridge University Press, 2008.
3. G. Li, G. Hu, H. Zhou, X. Fan, X. Li, “Attractive microwave-absorbing properties of $\text{La}_{1-x}\text{Sr}_x\text{MnO}_3$ manganite powders”, *Mater. Chem. Phys.*, **75** (2002) 101–104.
4. P. Galizia, I.V. Ciuchi, D. Gardini, C. Baldisserrri, C. Galassi, “Bilayer thick structures based on $\text{CoFe}_2\text{O}_4/\text{TiO}_2$ composite and niobium-doped PZT obtained by electrophoretic deposition”, *J. Eur. Ceram. Soc.*, **36** (2016) 373–380.
5. H. Su, X. Tang, H. Zhang, Y. Jing, F. Bai, “Low-loss magneto-dielectric materials: Approaches and developments”, *J. Electron. Mater.*, **43** (2014) 299–307.
6. P.J. Gogoi, M.M. Rabha, S. Bhattacharyya, N.S. Bhattacharyya, “Miniaturization of body worn antenna using nano magneto-dielectric composite as substrate in C-band”, *J. Magn. Magn. Mater.*, **414** (2016) 209–218.
7. P. Galizia, D. Gardini, S. Ortelli, C. Capiani, M. Anbinderis, R. Grigalaitis, G. Maizza, C. Galassi, “Novel magnetodielectric cobalt ferrite-titania-silica ceramic composites with tunable dielectric properties”, *Ceram. Int.*, **42** (2016) 16650–16654.
8. L.B. Kong, Z.W. Li, L. Liu, R. Huang, M. Abshinova, Z.H. Yang, C.B. Tang, P.K. Tan, C.R. Deng, S. Matitsine, “Recent progress in some composite materials and structures for specific electromagnetic applications”, *Int. Mater. Rev.*, **58** (2013) 203–259.
9. M. Aldrigo, D. Bianchini, A. Costanzo, D. Masotti, C. Galassi, “Exploitation of a novel magneto-dielectric substrate for miniaturization of wearable UHF antennas”, *Mater. Lett.*, **87** (2012) 127–130.
10. R.V. Petrov, A.S. Tatarenko, G. Srinivasan, J.V. Mantese, “Antenna miniaturization with ferrite ferroelectric composites”, *Microw. Opt. Techn. Lett.*, **50** (2008) 3154–3157.
11. R.C. Hansen, M. Burke, “Antennas with magneto-dielectrics”, *Microw. Opt. Technol. Lett.*, **26** (2000) 75–78.
12. Z. Zheng, H. Zhang, Q. Yang, L. Jia, J.Q. Xiao, “Low loss NiZn spinel ferrite-W-type hexaferrite composites from BaM addition for antenna applications”, *J. Phys. D: Appl. Phys.*, **47** (2014) 115001.
13. Z. Zheng, H. Zhang, Q. Yang, L. Jia, “Enhanced high-frequency properties of NiZn ferrite ceramic with Co_2Z -hexaferrite addition”, *J. Am. Ceram. Soc.*, **97** (2014) 2016–2019.
14. Q. Xia, H. Su, T. Zhang, J. Li, G. Shen, H. Zhang, X. Tang, “Miniaturized terrestrial digital media broadcasting antenna based on low loss magneto-dielectric materials for mobile handset applications”, *J. Appl. Phys.*, **112** (2012) 043915.
15. S. Banerjee, P. Hajra, A. Datta, A. Bhaumik, M.R. Mada, S. Bandyopadhyay, D. Chakravorty, “Magnetodielectric effect in $\text{Ni}_{0.5}\text{Zn}_{0.5}\text{Fe}_2\text{O}_4\text{-BaTiO}_3$ nanocomposites”, *Bull. Mater. Sci.*, **37** (2014) 497–504.
16. C.H. Henager Jr, J.L. Brimhall, L.N. Brush, “Tailoring structure and properties of composites synthesized in situ using displacement reactions”, *Mater. Sci. Eng. A*, **195** (1995) 65–74.
17. D. Hull, T.W. Clyne, *An Introduction to Composite Materials*, Cambridge University Press, 2007.
18. R.F. Gibson, T.-W. Chou, P.K. Raju, “Innovative processing and characterization of composite materials” presented at 1995 ASME International Mechanical Engineering Congress and Exposition, American Society of Mechanical Engineers, San Francisco, California, USA, 1995.
19. D.D.L. Chung, *Composite Materials Science and Applications*, Springer Science, 2010.
20. A.O. Karilainen, P.M. Ikonen, C.R. Simovski, S.A. Tretyakov, “Choosing dielectric or magnetic material to optimize the bandwidth of miniaturized resonant antennas”, *IEEE Trans Antennas Propag.*, **59** (2011) 3991–3998.
21. L.D. Zhang, H.F. Zhang, G.Z. Wang, C.M. Mo, Y. Zhang, “Dielectric behaviour of nano- TiO_2 bulks”, *Phys. Status Solidi A*, **157** (1996) 483–491.
22. P. Galizia, C. Baldisserrri, C. Capiani, C. Galassi, “Multiple parallel twinning overgrowth in nanostructured dense cobalt ferrite”, *Mater. Design*, **109** (2016) 19–26.
23. K. Haneda, A.H. Morrish, “Noncollinear magnetic structure of CoFe_2O_4 small particles”, *J. Appl. Phys.*, **63** (1988) 4258.
24. G.A. Samara, P.S. Peercy, “Pressure and temperature dependence of the static dielectric constants and raman spectra of TiO_2 (Rutile)”, *Phys. Rev. B*, **7** (1973) 1131.
25. M. Cernea, P. Galizia, I.V. Ciuchi, G. Aldica, V. Mihalache, L. Diamandescu, C. Galassi, “ CoFe_2O_4 magnetic ceramic derived from gel and densified by spark plasma sintering”, *J. Alloy Compd.*, **656** (2016) 854–862.
26. P. Galizia, G. Maizza, C. Galassi, “Heating rate dependence of anatase to rutile transformation”, *Process. Appl. Ceram.*, **10** (2016) 235–241.
27. P. Galizia, C. Baldisserrri, C. Galassi, “Microstructure development in novel titania-cobalt ferrite ceramic materials”, *Ceram. Int.*, **42** (2016) 2634–2641.
28. S. Jones, B. Lake, *United States Patent*, US 2008/0280150 A1, 2008.
29. P. Galizia, *Production and Morphological and Microstructural Characterization of Bulk Composites or Thick Films for the Study of Multiphysics Interactions*, PhD Thesis, Politecnico di Torino, Turin 2017. doi:10.6092/polito/porto/2674672
30. <http://literature.cdn.keysight.com/litweb/pdf/16454-90020.pdf>
31. J.L. Snoek, “Dispersion and absorption in magnetic ferrites at frequencies above one Mc/s”, *Physica*, **14** (1948) 207–217.
32. M. Drofenik, A. Znidarsic, D. Makovec, “Influence of the addition of Bi_2O_3 on the grain growth and magnetic permeability of MnZn ferrites”, *J. Am. Ceram. Soc.*, **81** (1998) 2841–2848.
33. A.C.F.M. Costa, E. Tortella, M.R. Morelli, R.H.G.A. Kiminami, “Synthesis, microstructure and magnetic properties of Ni-Zn ferrites”, *J. Magn. Magn. Mater.*, **256** (2003) 174–182.
34. P. Galizia, C. Ciomaga, L. Mitoseriu, C. Galassi, “PZT-cobalt ferrite particulate composites: Densification and lead loss controlled by quite-fast sintering”, *J. Eur. Ceram.*

- Soc., **37** (2017) 161–168.
35. P. Galizia, M. Cernea, V. Mihalache, L. Diamandescu, G. Maizza, C. Galassi, “Easy batch-scale production of cobalt ferrite nanopowders by two-step milling: Structural and magnetic characterization”, *Mater. Design*, **130** (2017) 327–335.
36. A. López-Ortega, E. Lottini, C. de Julián Fernández, C. Sangregorio, “Exploring the magnetic properties of cobalt-ferrite nanoparticles for the development of a rare-earth-free permanent magnet”, *Chem. Mater.*, **27** (2015) 4048–4056.
37. F.E. Carvalho, L.V. Lemos, A.C.C. Migliano, J.P.B. Machado, R.C. Pullar, “Structural and complex electromagnetic properties of cobalt ferrite (CoFe_2O_4) with an addition of niobium pentoxide”, *Ceram. Int.*, **44** (2017) 915–921.
38. K. Wagner, “Zur theorie der unvollkommenen dielektrika”, *Ann. Phys.*, **345** (1913) 817–855.
39. C.G. Koops, “On the dispersion of resistivity and dielectric constant of some semiconductors at audiofrequencies”, *Phys. Rev.*, **83** (1951) 121.
40. M.L.S. Teo, L.B. Kong, Z.W. Li, G.Q. Lin, Y.B. Gan, “Development of magneto-dielectric materials based on Li-ferrite ceramics: II. DC resistivity and complex relative permittivity”, *J. Alloys Compd.*, **459** (2008) 567–575.
41. A. Verma, D.C. Dube, “Processing of nickel-zinc ferrites via the citrate precursor route for high-frequency applications”, *J. Am. Ceram. Soc.*, **88** (2005) 519–523.
42. N. Sivakumar, A. Narayanasamy, B. Jeyadevan, R.J. Joseyphus, C. Venkateswaran, “Dielectric relaxation behaviour of nanostructured Mn-Zn ferrite”, *J. Phys. D: Appl. Phys.*, **41** (2008) 245001.
43. Z.L. Zheng, H.W. Zhang, J.Q. Xiao, L.J. Jia, F.M. Bai, “Introduction of NiZn-Ferrite Into Co(2)Z-ferrite and effects on the magnetic and dielectric properties”, *IEEE Trans. Magn.*, **48** (2012) 3618–3621.
44. D. Souriou, J.L. Mattei, S. Boucher, A. Sharaiha, A.C. Tarot, A. Chevalier, P. Queffelec, “Antenna miniaturization and nanoferrite magneto-dielectric materials”, *14th International Symposium on Antenna Technology and Applied Electromagnetics & the American Electromagnetics Conference (ANTEM-AMEREM)*, 2010.
45. C. Niamien, S. Collardey, K. Mahdjoubi, “Printed antennas over lossy magneto-dielectric substrates”, *4th European Conference on Antennas and Propagation*, Barcelona, Spain, 2010.